

Thermo-hydrodynamic Lubrication of Misaligned Porous Journal Bearings

Basim A. Abass
Asst.Prof.
Mushrek A. Mahdi
University of Babylon/
College of Engineering/
Dept of Mechanical Engineering\Iraq

Abstract

In this work, a numerical simulation for the thermo-hydrodynamic self-lubrication of misaligned porous circular journal bearing has been investigated. Mathematical model consists of a modified Reynolds equation to determine the pressure field of thin viscous oil film taking into account the oil leakage into the porous matrix, Darcy's law to determine the fluid flow in the porous media and the energy and the heat conduction equations to determine the temperature field in oil film thickness and the bearing shaft. The equation used to evaluate the oil film thickness was modified to include the effect of the bearing misalignment. The governing equations with appropriate boundary conditions were simultaneously solved using finite difference approach. Direct iterative procedure with successive under relaxation has been adopted through the present work. The effects of the dimensionless permeability and misalignment parameters on the performance characteristics of porous journal bearing have been presented and discussed. The results obtained from this analysis indicate that bearing performance is greatly affected by such parameters. The mathematical model as well as the computer program prepared to solve the governing equations of the present work have been verified by comparing the results of the load carrying capacity and attitude angle obtained through this work with that obtained by Boubendir et al.. Good agreement between the results has been obtained with maximum deviations of 4.8% and 4% respectively

Keywords: Thermo-hydrodynamic lubrication, Self-lubricating journal bearing, Misalignment effect.

1-Introduction

Self-lubricated bearings include a porous material filled with lubricating oil so that the bearing requires no further lubrication during the whole life of the machine. The self-lubricated bearings or oil retaining bearings exhibit this

feature. Self-lubricated porous bearings have the advantage of high production rate because short sintering time is required, N.B. Nadvana [1]. Porous journal bearings are widely used in industrial applications where other plain metal bearings are impractical

due to the lack of space or inaccessible to lubrication, like domestic appliances, medical apparatus, computers, automobiles. Lin and Hwang [2] applied the Brinkman extended Darcy's model to analyze the hydrodynamic lubrication of short porous journal bearings. Kaneko et al. [3] investigated theoretically the static characteristics at start of the operation in porous journal bearing with sealed ends lubricated only by the oil initially provided with its pores. Elsharkawy and Guedour [4] investigated a numerical solution for the hydrodynamic lubrication of finite porous journal bearings using a modified Brinkman-extended Darcy's model. Ertugrul [5] investigated experimentally the behavior of porous bearing under different lubricants and lubricating conditions. Abass, et al. [6] obtained theoretically the static characteristics of porous floating ring journal bearing under hydrodynamic lubrication condition when operating with improved boundary conditions. Marian, et al. [7] investigated rigorously two theoretical mass-conservative models for the tribological evaluation of porous journal bearings. Boubendir, et al. [8,9] studied numerically the thermo-hydrodynamic lubrication in

self-lubricating porous journal bearings. Their results performed that the thermal effects are non-negligible. An attempt has been prepared by Patel [10] to investigate the performance of a hydrodynamic short porous journal bearing under the presence of a magnetic fluid lubricant. Balasoiu, et al. [11] studied a 3D, isothermal numerical analysis of a cylindrical porous journal bearing characterized by a self-circulating lubricating system that eliminates the necessity of an external circulating pump. Rao, et al. [12] investigated the influence of surface porous layer configuration for a journal bearing with double layer porous lubricant film.

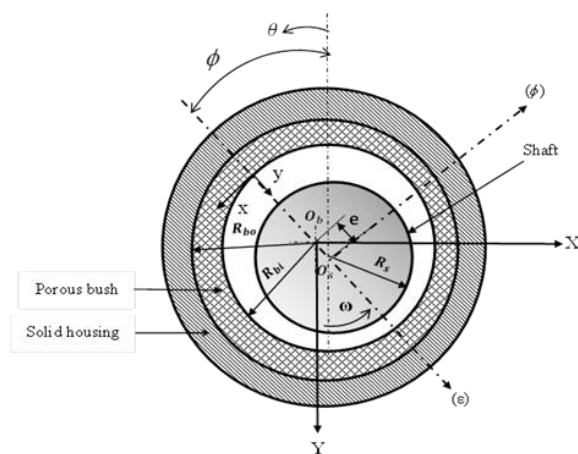
In most theoretical investigations of hydrodynamic lubrication it has been supposed that the journal and the bearing axis are aligned. Misalignment phenomenon is the root cause of many journal bearing failures. It is, however, difficult to avoid misalignment due to improper assembly, elastic and thermal distortions of the shaft and bearing housing. Therefore, it is important to consider misalignment when designing journal bearings. Most investigators in this area confined their work to solid bearing. Pinkus and Bupara [13] presented a comprehensive analysis of

misaligned bearings and charts which revealed some of the salient features of different misaligned journal. Safar [14] estimated the maximum allowable value of misalignment for a bearing with length to diameter ratio of unity. Safar and Raid, [15] studied the effect of misalignment on the performance characteristics of journal bearings operating in turbulent regime. Keith [16] analyzed a misaligned grooved journal bearing considered both types of misalignment; axial (vertical displacement) and twisting (horizontal displacement) by used the cavitation algorithm, which automatically predicts film rupture and reformation in bearings. Banwait and Patiala [17] studied the thermo-hydrodynamic lubrication of a misaligned journal bearing. Boedo and Booker [18] investigated transient and steady state behavior of grooveless (angularly) misaligned bearings with finite element formulations of the complete two-dimensional Reynolds equation. Bouyer and Fillon [19] studied the misaligned journal bearing theoretically and experimentally. Nikolakopoulos and Papadopoulos [20] developed an analytical model to find the relationship among the friction force, the misalignment

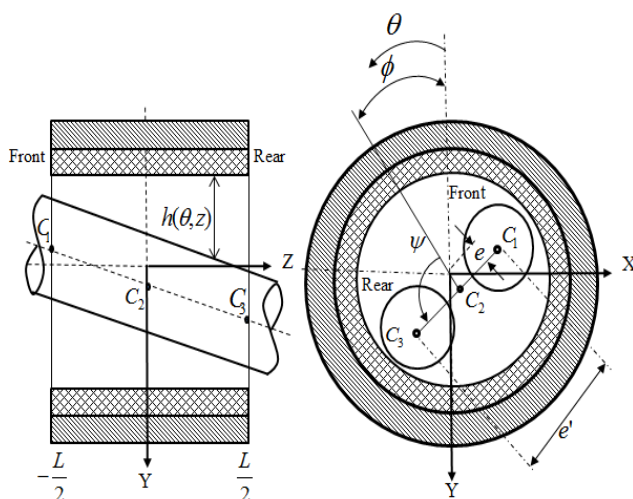
angles, and wear depth. Abbas and Kadim [21] investigated the influence of surface roughness on thermo-hydrodynamic performance in aligned and misaligned journal bearings by considering an average flow model and deriving the shear flow factor for various roughness configurations, similar to the pressure flow factor. He et al. [22] studied numerically the effects of journal misalignment caused by an asymmetric rotor structure on a journal bearing performance. In the present work the steady state thermo-hydrodynamic characteristics of the misaligned porous journal bearing has been investigated. The effect of different parameters affecting the thermal performance of the bearing such as the bearing permeability and degree of misalignment has been investigated. The modified Reynolds equation includes the filter velocity and temperature effects, Darcy's equation to determine the oil flow inside the porous material, the energy equation and the heat conduction equation have been solved simultaneously with suitable boundary conditions using finite difference technique.

2. Bearing Geometry and Governing Equations

The schematic diagram of a misaligned porous journal bearing considered in this work is given in fig.1. The shaft rotates at a constant angular velocity about its axis. The shaft radius (R_s) and the bearing radius (R_b) are practically identical



(a). Coordinate System.



(b). Misaligned Bearing.

Fig.(1). Geometrical Configuration of Misaligned porous Journal Bearing

3- Reynolds Equation:

The modified Reynolds equation of porous journal bearing for Newtonian, laminar, incompressible fluid flow including thermal effect condition in clearance space between surfaces of journal and porous bush is given by Boubendir et al.[8,9].

$$\frac{\partial}{\partial x} \left[\left(F_1 + \frac{K.F_2}{\mu} \right) \frac{\partial P}{\partial x} \right] + \frac{\partial}{\partial z} \left[\left(F_1 + \frac{K.F_2}{\mu} \right) + \frac{\partial P}{\partial z} \right] = U \frac{\partial}{\partial x} (h - F_2) - \frac{K}{\mu} \frac{\partial P^*}{\partial R_b} \Big|_{R=R_b} \quad (1)$$

$$F_1 = \int_0^h \frac{y}{\mu} (y - F_2) dy, \quad F_2 = \frac{F_3}{F_4}, \quad F_3 = \int_0^h \frac{y}{\mu} dy,$$

$$F_4 = \int_0^h \frac{dy}{\mu}$$

(2)

The porous material is assumed to be homogeneous and isotropic

4-Darcy's Equation

The fluid flow inside the porous media is governed by Darcy's law [3]

$$\frac{\partial^2 P^*}{\partial R_b^2} + \frac{1}{R_b} \frac{\partial P^*}{\partial R_b} + \frac{1}{R_b^2} \frac{\partial^2 P^*}{\partial \theta^2} + \frac{\partial^2 P^*}{\partial z^2} = 0 \quad (3)$$

The above equation is still valid only for a weak velocity with in the porous media.

5- Oil Film Thickness:

The oil film thickness for misaligned journal bearing system as shown in Fig. (1-b) can be introduced as [23]

$$h = c \left\{ (1 + \varepsilon \cos(\theta - \phi)) + \frac{z}{L} \varepsilon' \cos(\theta - \psi - \phi) \right\} \quad (4)$$

Where,

$$\varepsilon' = D_m \cdot \varepsilon'_{\max} \quad (5)$$

$$\varepsilon'_{\max} = 2 \left(\sqrt{1 - \varepsilon^2 \cdot \sin^2 \psi} - \varepsilon |\cos \psi| \right) \quad (6)$$

6-Energy Equation

The energy equation is used to calculate the oil film temperature in clearance region with considered steady state lubricant ,Newtonian ,laminar flow and an incompressible, this equation is given by [8,10]:

$$\rho C_p \left(u \frac{\partial T}{\partial x} + v \frac{\partial T}{\partial y} + w \frac{\partial T}{\partial z} \right) = K_f \left(\frac{\partial^2 T}{\partial y^2} \right) + \mu \left[\left(\frac{\partial^2 u}{\partial y^2} \right) + \left(\frac{\partial^2 w}{\partial y^2} \right) \right] \quad (7)$$

7-Heat conduction equation-

Within the porous bush neglecting the convective effects(viscose effects), thus the heat conduction equation for the porous body can be written as [17]:

$$\frac{\partial^2 T_b}{\partial R_b^2} + \frac{1}{R_b} \frac{\partial T_b}{\partial R_b} + \frac{1}{R_b^2} \frac{\partial^2 T_b}{\partial \theta^2} + \frac{\partial^2 T_b}{\partial z^2} = 0 \quad (8)$$

8- Fluid-Film Velocity Components

The velocity field must be computed as it affects the convective and the dissipative terms of the energy equation. The velocity components for the flow lubricant in clearance gap in circumferential and axial directions, which are derived :[from the GRE, are as follows [9

$$u = \frac{\partial P}{\partial x} (F_5 - F_6 F_2) + (u_2 - u_1) \frac{F_6}{F_4} + u_1 \quad (9)$$

$$w = \frac{\partial P}{\partial z} (F_5 - F_6 F_2) + (w_2 - w_1) \frac{F_6}{F_4} + w_1 \quad (10)$$

Where ;

$$(11) \quad F_5 = \int_0^y \frac{y}{\mu} dy, \quad F_6 = \int_0^y \frac{dy}{\mu}$$

$$u_1 = - \frac{K}{\mu} \frac{\partial P^*}{\partial R_b} \Big|_{R_b=R_{bi}}, \quad u_2 = \omega R_s \quad (12)$$

$$w_1 = - \frac{K}{\mu} \frac{\partial P^*}{\partial z} \Big|_{R_b=R_{bi}}, \quad w_2 = 0 \quad (13)$$

The fluid- film velocity component across the fluid-film is obtained from the continuity equation and is expressed as :

$$v = - \int_0^y \left(\frac{\partial u}{\partial x} + \frac{\partial w}{\partial z} \right) dy \quad (14)$$

9-Viscosity –Temperature relationship

The Reynolds and energy equations are coupled by the oil

film viscosity which was assumed to be variable across the fluid film, around the circumference and in axial direction. The relationship between temperature and viscosity is given by [10]

$$(15) \quad \mu = \mu_o e^{-\beta_o(T-T_o)}$$

To generalize the study, the following non-dimensional coordinates and parameters can be defined :

$$P = \bar{P} \mu_o \omega \left(\frac{R_s R_b}{c^2} \right), \quad \bar{h} = \frac{h}{c}, \quad \bar{K} = \frac{K.c}{R_b}, \quad \bar{c} = \frac{c}{R_{bi}},$$

$$\theta = \frac{x}{R_{bi}}, \quad \bar{y} = \frac{y}{h}, \quad \bar{Z} = \frac{z}{L}, \quad \bar{R} = \frac{R}{R_{bi}}, \quad \bar{\mu} = \frac{\mu}{\mu_o}$$

$$u, v, w = \omega R_s (\bar{u}, \bar{v}, \bar{w})$$

Then the governing equations in non-dimensional form can be written as follow-:

Dimensionless Reynolds -
:equation

$$\frac{\partial}{\partial \theta} \left[\left(\bar{h}^3 \bar{F}_1 + \frac{\bar{K} \bar{c} \bar{h} \bar{F}_2}{\bar{\mu}} \right) \frac{\partial \bar{P}}{\partial \theta} \right] + \alpha^2 \frac{\partial \bar{P}}{\partial \bar{Z}} \left[\left(\bar{h}^3 \bar{F}_1 + \frac{\bar{K} \bar{c} \bar{h} \bar{F}_2}{\bar{\mu}} \right) \frac{\partial \bar{P}}{\partial \bar{Z}} \right]$$

$$= \frac{\partial}{\partial \theta} \left(\bar{h} (1 - \bar{F}_2) \right) - \frac{\bar{K}}{\bar{\mu}} \frac{\partial \bar{P}^*}{\partial \bar{R}_b} \Bigg|_{\bar{R}=1} \quad (16)$$

-Dimensionless Darcy's equation:

$$\frac{\partial^2 \bar{P}^*}{\partial \bar{R}_b^2} + \frac{1}{\bar{R}_b} \frac{\partial \bar{P}^*}{\partial \bar{R}} + \frac{1}{\bar{R}_b^2} \frac{\partial^2 \bar{P}^*}{\partial \theta^2} + \alpha^2 \frac{\partial^2 \bar{P}^*}{\partial \bar{Z}^2} = 0 \quad (17)$$

-Dimensionless oil film thickness:

$$\bar{h} = 1 + \varepsilon \cos(\theta - \phi) + \bar{Z} \varepsilon' \cos(\theta - \phi - \phi) \quad (18)$$

-Dimensionless energy equation :

$$P_e \left[\bar{u} \frac{\partial \bar{T}}{\partial \theta} + \left(\frac{\bar{v}}{\bar{c} \bar{h}} - \bar{u} \frac{\bar{y}}{h} \frac{\partial \bar{h}}{\partial \theta} - \alpha \bar{w} \frac{\partial \bar{h}}{\partial \bar{Z}} \right) \frac{\partial \bar{T}}{\partial \bar{y}} + \alpha \bar{w} \frac{\partial \bar{T}}{\partial \bar{Z}} \right] = \frac{\partial^2 \bar{T}}{\partial \bar{y}^2} + \frac{\bar{\mu}}{\bar{h}^2} N_d \left[\left(\frac{\partial \bar{u}}{\partial \bar{y}} \right)^2 + \left(\frac{\partial \bar{w}}{\partial \bar{y}} \right)^2 \right] \quad (19)$$

$$\text{Where, } P_e = \frac{\rho c_p U c^2}{K_f R_{bi}}, \quad N_d = \frac{\mu_o U^2}{K_f T_o}$$

-Dimensionless heat conduction equation:

$$\frac{\partial^2 \bar{T}_b}{\partial \bar{R}_b^2} + \frac{1}{\bar{R}_b} \frac{\partial \bar{T}}{\partial \bar{R}_b} + \frac{1}{\bar{R}_b^2} \frac{\partial^2 \bar{T}}{\partial \theta^2} + \alpha^2 \frac{\partial^2 \bar{T}}{\partial \bar{Z}^2} = 0 \quad (20)$$

-Dimensionless viscosity-
temperature equation:

$$\bar{\mu} = e^{-\beta T_o (\bar{T}-1)} \quad (21)$$

- Dimensionless fluid-film
velocity components:

$$\bar{u} = \frac{u}{\omega R_s} = \frac{\partial \bar{P}}{\partial \theta} \left[\frac{\bar{h}^2 (\bar{F}_5 - \bar{F}_6 \bar{F}_2)}{2} + \frac{\bar{K} \bar{c}}{\bar{\mu}} \left(\frac{\bar{F}_6}{\bar{F}_4} - 1 \right) \right] + \frac{\bar{F}_6}{\bar{F}_4}$$

$$\bar{w} = \frac{w}{\omega R_s} = \frac{\partial \bar{P}}{\partial \bar{Z}} \left[\frac{\bar{h}^2 (\bar{F}_5 - \bar{F}_6 \bar{F}_2)}{2} + \frac{\bar{K} \bar{c}}{\bar{\mu}} \left(\frac{\bar{F}_6}{\bar{F}_4} - 1 \right) \right] \quad (23)$$

$$\bar{v} = -\bar{h} \bar{c} \int_0^{\bar{y}} \left(\frac{\partial \bar{u}}{\partial \theta} - \frac{\bar{y}}{h} \frac{\partial \bar{h}}{\partial \theta} \frac{\partial \bar{u}}{\partial \bar{y}} + \alpha \frac{\partial \bar{w}}{\partial \bar{z}} - \alpha \frac{\bar{y}}{h} \frac{\partial \bar{h}}{\partial \bar{z}} \frac{\partial \bar{w}}{\partial \bar{y}} \right) d\bar{y} \quad (24)$$

10 Boundary Condition:

The following boundary conditions are used to gather with the governing equations to analyze the problem of thermo-

hydrodynamic performance of misaligned porous journal bearing:

A). Lubricant flow field:

1- At the journal bearing edges

$$\bar{P}(\theta, 0.5) = \bar{P}(\theta, -0.5) = 0$$

2- At the Cavitation zone ;

$$\bar{P}(\theta, \bar{Z}) = 0, \quad \frac{\partial \bar{P}}{\partial \theta}(\theta, \bar{Z}) = 0$$

3-At the outer surface of porous bush ($\bar{R}_b = R_{bo}/R_{bi}$)

$$\frac{\partial \bar{P}^*}{\partial R_b}(\theta, \bar{R}_b, \bar{Z}) = 0$$

4- At the porous bearing edges ;

$$\frac{\partial \bar{P}^*}{\partial R_b}(\theta, \bar{R}_b, \pm 0.5) = 0$$

5-At the porous bush-fluid film interface

$$\bar{P}^*(\theta, 1, \bar{Z}) = \bar{P}(\theta, \bar{Z})$$

B). Thermal field

1- The temperature distribution through the oil film and porous domain can be determined by solving the energy equation and heat conduction equation subjected to the following boundary conditions :

2- The temperature of outer surface of porous bush given by [8]:

$$T_b|_{R_b=R_{bo}} = T_a = 45C^o \Rightarrow$$

$$\bar{T}_b|_{\bar{R}_b=R_{bo}/R_{bi}} = \frac{T_b|_{R_b=R_{bo}}}{T_o} = \frac{T_a}{T_o} = 1.125 \quad (25)$$

The temperature of porous bearing at the axial ends given by [8] .

$$T_b|_{Z=\pm \frac{L}{2}} = T_a = 45C^o \Rightarrow$$

$$\bar{T}_b|_{\bar{Z}=\pm 0.5} = \frac{T_b|_{Z=\pm \frac{L}{2}}}{T_o} = \frac{T_a}{T_o} = 1.125 \quad (26)$$

3-The heat flux continuity on the surface between the porous bush and the oil film interface which yield to the followed as described by [8,9]

$$T|_{y=0} = T_b|_{R_b=R_{bi}} \Rightarrow \bar{T}|_{y=0} = \bar{T}_b|_{\bar{R}_b=1}$$

$$K_b \frac{\partial T_b}{\partial R_b} \Big|_{R_b=R_{bi}} = -K_f \frac{\partial T}{\partial y} \Big|_{y=0} \Rightarrow$$

$$K_b \frac{\partial \bar{T}_b}{\partial \bar{R}_b} \Big|_{\bar{R}_b=1} = -\frac{K_f}{c.h} \frac{\partial \bar{T}}{\partial y} \Big|_{y=0} \quad (27)$$

4- The shaft temperature in the sliding direction is supposed to be constant by applying zero flux boundary condition. It is determined by averaging temperature in the adjacent lubricant layer as [24]:

$$\bar{T}_s = \frac{1}{2\pi} \int_0^{2\pi} \bar{T} \Big|_{y=1} d\theta \quad (28)$$

11-Bearing Parameters:

The components of the load carrying capacity along and perpendicular to the line of centers are calculated as the following non-dimensional parameters [9,21]:

$$\bar{W}_\varepsilon = \frac{c^2 W_\varepsilon}{\mu_o U R_{bi}^2 L} = \int_{-0.5}^{0.5} \int_0^{2\pi} \bar{P} \cdot \cos(\theta) \cdot d\theta \cdot d\bar{z} \quad (29)$$

$$\bar{W}_\phi = \frac{c^2 W_\phi}{\mu_o U R_{bi}^2 L} = \int_{-0.5}^{0.5} \int_0^{2\pi} \bar{P} \cdot \sin(\theta) \cdot d\theta \cdot d\bar{z} \quad (30)$$

The total load carrying capacity of the bearing can be evaluated as:

$$\bar{W} = \frac{c^2 W}{\mu_o UR_{bi}^2 L} = \sqrt{\bar{W}_\varepsilon^2 + \bar{W}_\phi^2} \quad (31)$$

The attitude angle is [9]

$$\phi = \tan^{-1} \left(-\frac{\bar{W}_\phi}{\bar{W}_\varepsilon} \right) \quad (32)$$

The required moment for steady state operation is calculated directly from the fluid film pressure distribution. Two components of the moment vector are required [17]-:

$$\bar{M}_\varepsilon = \frac{c^2 M_\varepsilon}{\mu_o UR_{bi}^2 L^2} = \int_{-0.5}^{0.5} \int_0^{2\pi} \bar{P} \cdot \bar{z} \cdot \cos(\theta) \cdot d\theta d\bar{z} \quad (33)$$

$$\bar{M}_\phi = \frac{c^2 M_\phi}{\mu_o UR_{bi}^2 L^2} = \int_{-0.5}^{0.5} \int_0^{2\pi} \bar{P} \cdot \bar{z} \cdot \sin(\theta) \cdot d\theta d\bar{z} \quad (34)$$

And the total moment in dimensionless form can be calculated as follows :

$$\bar{M} = \sqrt{\bar{M}_\varepsilon^2 + \bar{M}_\phi^2} \quad (35)$$

The velocity component of the oil film along the axial direction is the key factor in the oil flow leakage. The dimensionless side leakage flow is determined by using the following relation

$$\bar{Q}_s = \frac{Q_s L}{c\omega R_s^2} = \int_0^{2\pi} \int_0^1 \bar{h}\bar{w} \Big|_{z=\pm 0.5} d\bar{y} d\theta \quad (36)$$

12-Solution Procedure

Thermo-hydrodynamic analysis of misaligned self-lubricated porous journal bearing required the simult-

aneous solution of governing equations with appropriate boundary conditions. These equations are numerically solved using the finite difference approach. Iterative procedure with successive under relaxation has been used to obtain the pressure and temperature distributions in the oil film and porous matrix. The solution procedure is as follows:

1-Select the operating conditions, characteristic properties, initial pressure and temperature distributions of the oil film and the porous matrix. Compute initial value of attitude angle as:

$$\phi = \tan^{-1} \left(\frac{\pi \sqrt{1-\varepsilon^2}}{4 \varepsilon} \right) \quad (37)$$

2-Evaluate the viscosity distribution and the values of the viscosity integrals ($\bar{F}_1, \bar{F}_2, \bar{F}_3, \bar{F}_4, \bar{F}_5, \bar{F}_6$).

3-Compute the film thickness using equation (18).

4-The oil pressure inside the porous bush is calculated by solving Laplace (Darcy's) equation (17) for the porous matrix. The iterations stopped if convergence criterion reaches (10^{-4})

5-New pressure distribution can be obtained by an iterative solution of the modified Reynolds equation (16) with successive under relaxation using appropriate boundary

conditions of the lubricant flow field. The iteration is stopped when the pressure convergence criterion reaches (10^{-4}) . New value of attitude angle can be calculated from equation (32). The old and new attitude angle is compared. The iteration is stopped when the attitude angle convergence criterion reaches (10^{-4}) . The velocity components can be calculate using equations (22, 23and 24)

6-The energy equation (19) and heat conduction equation (20) with the boundary conditions are solved simultaneously. The new oil-film temperature is used to compute a new viscosity field in step (2) which is subsequently used to solve the Reynolds equation and simultaneous solutions for the equations are obtained iteratively until the convergence criterion of the temperature for all points on the boundary between the oil film and the inner bush face is less than (10^{-6}) . A computer program written in Fortran-90 has been prepared to solve the governing equations of the problem. Figure (A-1) shows the program flow chart .

13- Results and Discussion:

The results obtained through this work have been obtained for a porous journal bearing with the geometric and operating parameters presented in table (1). The effect porous bearing permeability on the load carrying capacity and attitude angle for aligned porous journal bearing have been compared to that obtained by Boubendir et al. [8] as shown in Figs. (2) and (3). The maximum deviation of the results for load carrying capacity and attitude angle have been calculated and found to be 4.8%, 4% respectively. It appears from these figures that the results are in a good agreement. The above comparison characterizes a good verification to the mathematical model as well as the computer program used to solve the governing equations in the present work.

Table 1: Technical data used for numerical simulation[8]

Bearing length			
$L = 0.044$ m			
Radial clearance			
$c = 0.0000825$ m			
Shaft radius			
$R_s = 0.0275$ m			
Internal bearing radius			
$R_{bi} = 0.02758$ m			
External bearing radius			
$R_{bo} = 0.05$ m			
Eccentricity Ratio			$\varepsilon = 0.8$
Dimensionless permeability			parameter
$\bar{K} = 0.0001, 0.01, 1$			

Degree of misalignment
 $D_m = 0.4, 0.8, 0.9$
 Angle between the journal rear centerline
 $\psi = 0^\circ, 90^\circ$
 projection and the eccentricity vector
 Initial lubricant temperature $T_o =$
 $40^\circ C$
 Rotation speed
 $N = 2500rpm$
 Lubricant density
 $\rho = 8600 \text{ kg/m}^3$
 Inlet lubricant viscosity
 $\mu_o = 0.032 \text{ pa}\cdot\text{sec}$
 Thermo-viscous parameter
 $\beta = 0.034$
 Lubricant specific heat
 $C_p = 2000 \text{ J/kg}\cdot^\circ C$
 Lubricant thermal conductivity
 $K_f = 0.13 \text{ W/m}\cdot^\circ C$ Bush thermal conductivity
 $K_b = 38 \text{ W/m}\cdot^\circ C$

The results presented in Figs. (4-9) have been obtained for a porous bearing working at misalignment parameters ($D_m = 0.8, \psi = 90^\circ$) and for different values of dimension-nless permeability parameters. Fig.(4) shows the variation of the oil film pressure for a misaligned porous bearing with the circumferential direction at the mid-plane of the bearing. It is found that the increasing of the permeability parameter produces a reduction in the oil film pressure which can be explained from the oil migration into the porous matrix which reduces the oil content in clearance gap. A reduction in oil film pressure of 41.2% has been calculated for a porous bearing that has permeability parameter (\bar{K}) of 0.01 than that has $\bar{K} = 0.0001$. Fig.(5) describes the variation of the dimensionless oil film temperature distributions in

circumferential direction at the mid-plane of misaligned porous journal bearing that has different permeability parameters and eccentricity ratio of 0.8. It can be observed from this figure that, increasing the bearing permeability has a little effect (reduction) in oil film temperature. A decrease of 1.5% in maximum oil film temperature has been noticed for the porous bearing that has $\bar{K} = 0.0001$ that has $\bar{K} = 1$. This is can be attributed to the fact that the flow is free to move for the bearing with high permeability, and the decrease of the velocity components (due to the decrease of the oil film pressure). The effect of the bearing permeability on the dimensionless load carry-ing capacity and misalignment moment is presented in Figs.(6 and 7). It can be seen from these figures, that both load carrying capacity and misalignment moment of the bearing are highly affected by the bearing permeability when working at higher eccentricity ratio and higher permeability parameter. This is expected since both the bearing load carrying capacity and the misaligned moment are functions of oil film pressure. Fig.(8) depicts that the attitude angle decreases with the increase of the bearing eccentricity ratio while it increases for the bearing that has higher permeability parameter. A increase of 8% in attitude angle has been obtained for a porous journal bearing that has $\bar{K} = 1$ than that has $\bar{K} = 0.0001$ working at eccentricity

ratio of 0.7 while it becomes 20% for the same bearing working at eccentricity ratio of 0.8. The influence of permeability on the dimensionless side leakage flow of a misaligned porous journal bearing is described in Fig (9). It can be shown from this figure that there is a little decrease in the side leakage flow for the porous journal bearing that has higher permeability parameter spatially when it works at higher eccentricity ratios. The percentage of reduction in side leakage flow has been calculated and found to negligible when the bearing permeability increases from 0.0001 to 0.01 for the bearing working at eccentricity ratio of 0.7 while it becomes 21% when the bearing permeability increases from 0.0001 to 1 at the working conditions. . This is can be attributed to the decreases of the achieved oil film pressure and then the pressure gradient at the bearing ends section. Fig. 10(a-d) displays the variation of oil film thickness in circumferential direction for aligned and misaligned porous journal bearing working at $\varepsilon=0.8$ and different values of misalignment parameters. Fig. 10(a) illustrates the oil film thickness at the front side of the porous journal bearing. This figure obviously shows that the minimum oil film thickness of the front side of bearing becomes larger as the journal bearing works at higher misalignment parameters (D_m). This indicates that the oil film thickness inclines to one side, while the oil film thickness of the rear side

decreases leads to serious metal to metal contact as can be shown in Fig. 10(b). The effect of the angle ψ when it becomes 90° can be shown in Fig. 10(c and d). It is clear that the minimum oil film thickness at the front and the rear sides of the bearing decreases as the bearing working at higher misalignment degree D_m . It can also be shown from this figure that the position of the minimum oil film thickness occurs at different positions for the bearing that has $\psi=0^\circ$ and $\psi=90^\circ$. For example the position of minimum oil film thickness of a bearing that has $\psi=0^\circ$ locates at $\theta=202^\circ$ for both cases of rear and front of the bearing while the position differs with the bearing permeability for the bearing with $\psi=90^\circ$. The results presented in Figs. (11 to 16) have been obtained for a porous journal bearing with permeability parameter (0.001). The variation of axial and circumferential dimensionless oil film pressure for the aligned and misaligned porous journal bearing operating at $\varepsilon=0.8$ is depicted in Fig. 11(a-g). Fig. 11(a) shows the oil film pressure for the aligned porous bearing which is found to be symmetrical along the bearing width. The misalignment parameters, namely, D_m and ψ influence the oil film pressure distribution and changes its shape. Fig. 11(b,c) shows the oil film pressure when $D_m=0.4$ and $\psi=0^\circ$ and 90° . It is clear from this figure that the oil film pressure is slightly

affected by the misalignment of the journal in this case. Fig.11(d) shows that the maximum oil film pressure of the porous bearing inclines to the rear side of bearing due to the reduction of the oil film thickness in this side when $\psi = 0^\circ$ and $D_m = 0.8$. Fig. 11(e) shows that the pressure profile has a two unsymmetrical pressure spikes at both front and rear sides of the bearing when it works with $\psi = 90^\circ$ and $D_m = 0.8$. While in Fig. 11(f) a higher maximum oil film pressure (12.744) is located at the rear side of the porous bearing when the porous journal bearing works at $D_m = 0.9$ and $\psi = 0^\circ$. This is because the drastically reduction of the oil film thickness in this side of bearing in this case. A low pressure spikes become clearer at the ends of the bearing working at $D_m = 0.9$ and $\psi = 90^\circ$ as shown in Fig. 11(g). Fig. (12) shows the variation of dimensionless oil film temperature distribution along the circumferential direction at the mid-plane of porous journal bearing that has a permeability parameter of 0.001 and working at different misalignment degree. It can be observed from this figure that, increasing of D_m causes a slight increase in oil film temperature for both case of ψ . The maximum oil film temperature increases by about 2.3% when the porous bearing works at $D_m = 0.9$ and $\psi = 90^\circ$ in comparison with the aligned bearing. The variation of dimensionless load carrying capacity and misalignment moment with

eccentricity ratio for aligned and misaligned porous journal bearing is illustrated in Figs. (13 and 14). It is found that for both cases when $\psi = 0^\circ$ and 90° an increase in load carrying capacity and misalignment moment has been obtained when the bearing works at higher misalignment degree D_m . It is clear from Fig.(13) that a slight increase in load carrying capacity has been observed when the porous bearing works at higher misalignment degree. The percentage of increase has been calculated and found to be 31.2% for a misaligned porous journal bearing working at 0.9 misalignment degree and $\epsilon = 0.65$ in comparison with the aligned one. This is can be attributed to the decrease in oil film thickness of the bearing in this case. Fig.(15) presented the variation of attitude angle with bearing eccentricity ratios for a bearing working at different values of misalignment parameters. It can also be shown from this figure that the attitude angle decreases when the bearing works at higher degree of misalignment for both cases when $\psi = 0^\circ$ and $\psi = 90^\circ$. The maximum percentage of decrease in attitude angle for a porous journal bearing works at 0.25 eccentricity ratio and $D_m = 0.9$ has been calculated and found to be 28.4% with that operating with $D_m = 0.4$. The variation of dimensionless side leakage flow with eccentricity ratio for the aligned and misaligned porous journal bearing that has a

permeability parameter $\bar{k} = 0.001$ has been presented in Fig.(16). It can be observed from this figure that the side leakage increases for the porous bearing works at higher degree of misalignment for both cases of ψ .

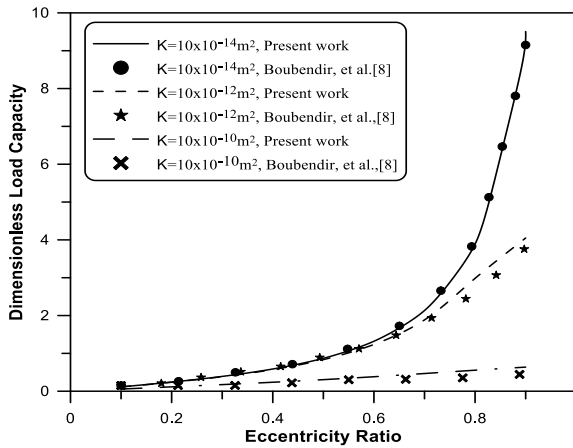


Fig.2. Load carrying capacity versus eccentricity ratio with different values of dimensionless permeability parameter.

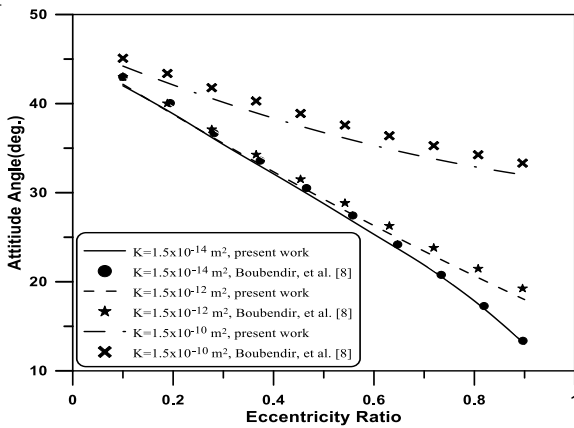


Fig. 3. Attitude angle versus eccentricity ratio for different values of dimensionless permeability parameter.

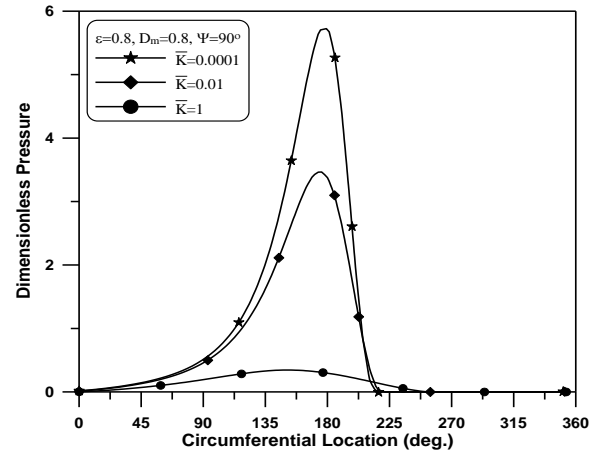


Fig. 4. Dimensionless oil film pressure (\bar{P}) along the circumferential direction for a misaligned bearing with different values of permeability parameter

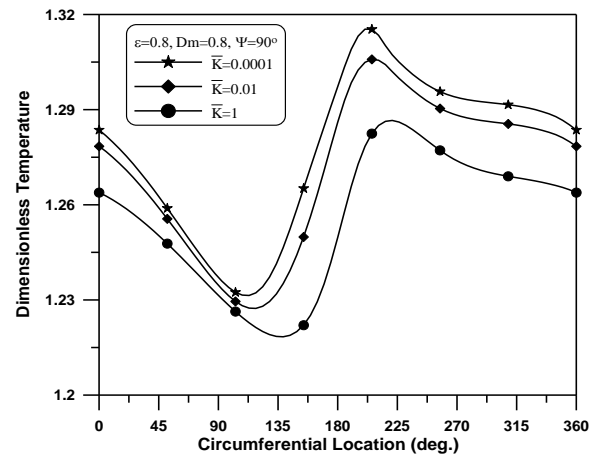


Fig. 5. Dimensionless oil film temperature (\bar{T}) in the circumferential direction for a misaligned porous bearing with different values of permeability parameter.

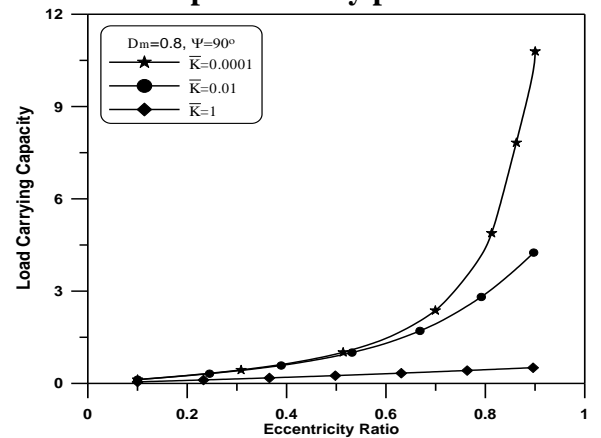


Fig. 6. Dimensionless load carrying capacity (\bar{W}) versus eccentricity ratio for

different values of permeability parameter.

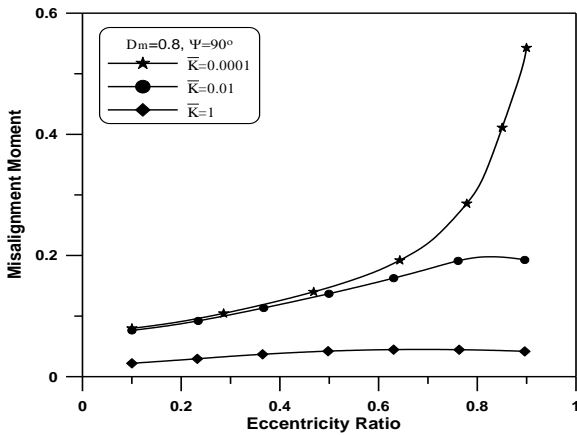


Fig. 7. Dimensionless misalignment moment (\bar{M}) versus eccentricity ratio for different values of permeability parameter.

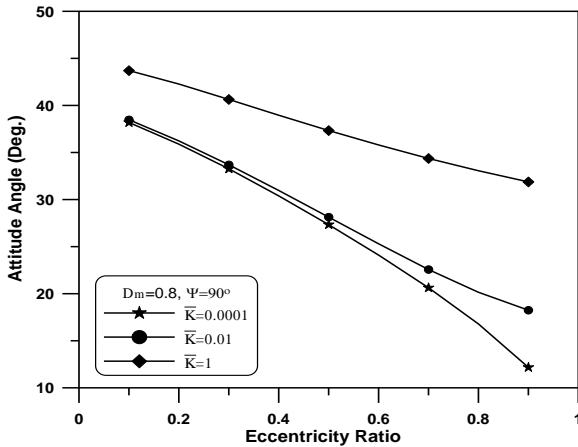


Fig. 8. Attitude angle (ϕ) versus eccentricity ratio with different values of permeability parameter.

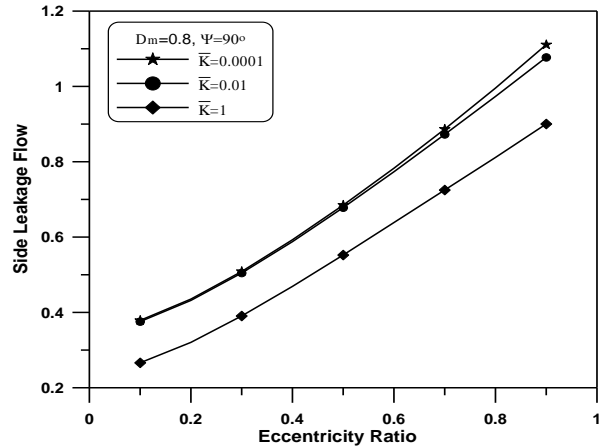
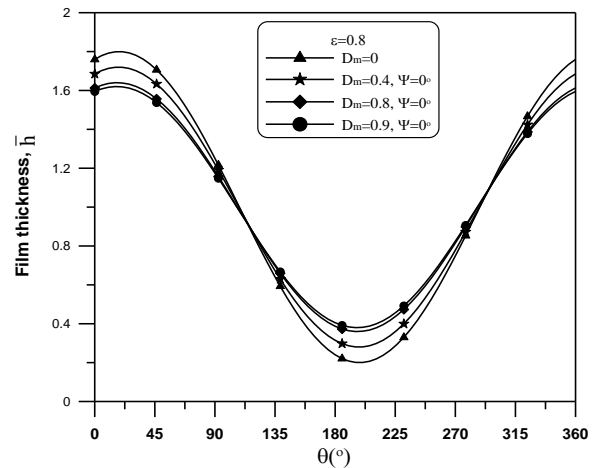
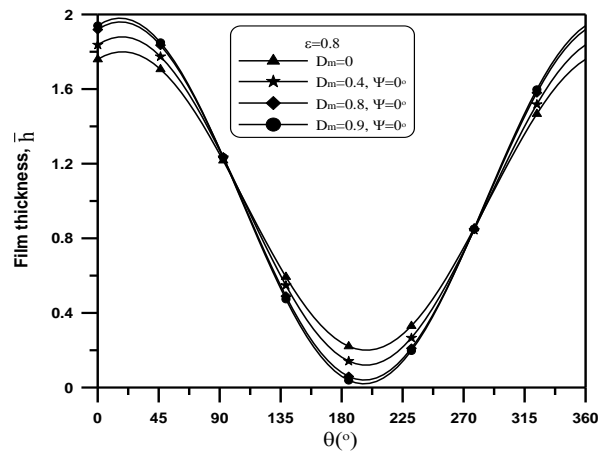


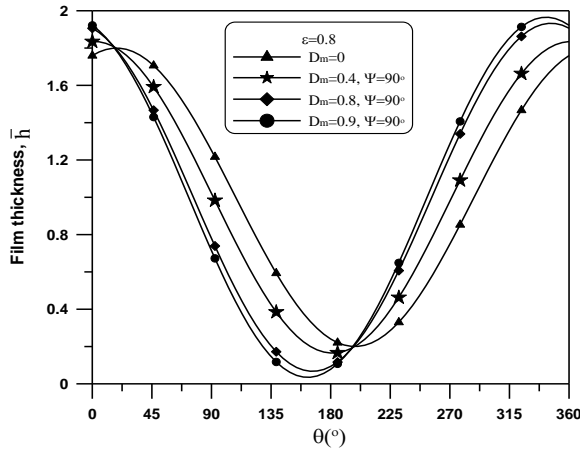
Fig. 9. Dimensionless side leakage flow (\bar{Q}_s) versus eccentricity ratio for a misaligned porous bearing with different values of permeability parameter.



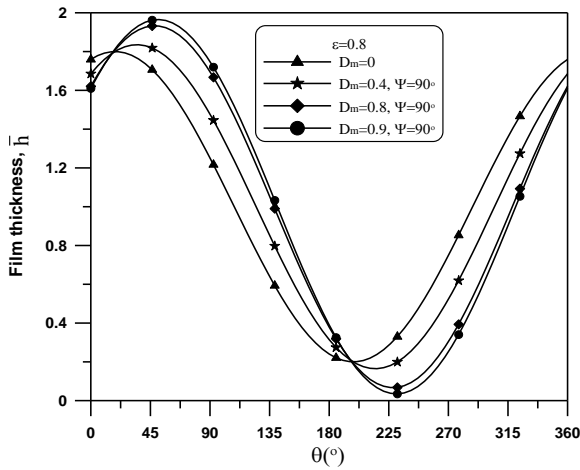
(a). Front Side



(b). Rear Side



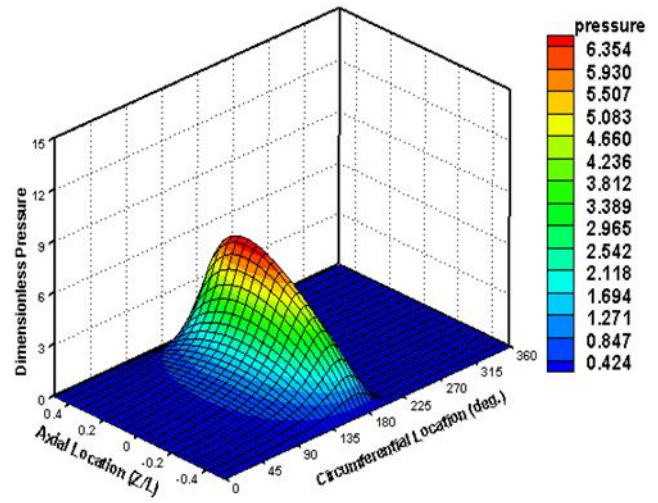
(c). Front Side



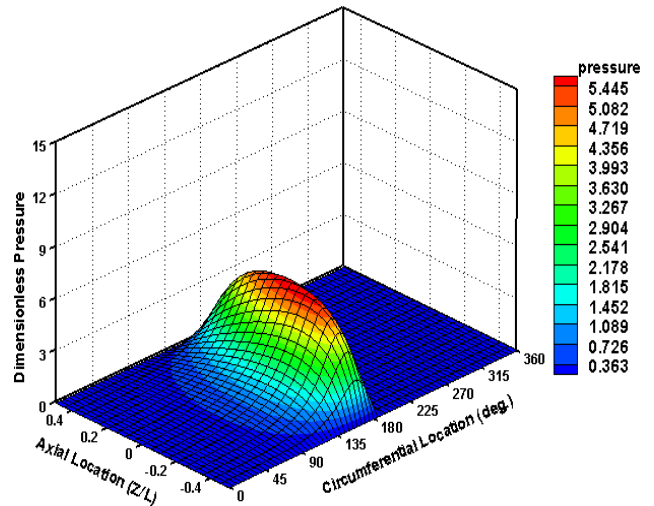
(d) Rear Side

Fig. 10. Variation of oil film thickness in the angular coordinate for different values of D_m at $\psi = 90^\circ$ and $\epsilon = 0.8$

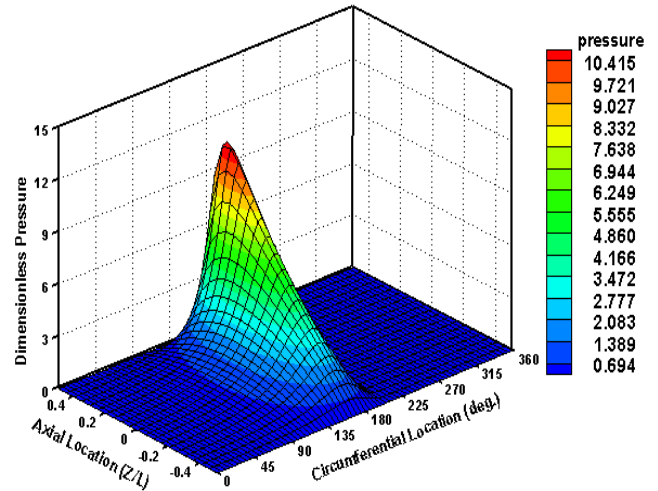
(a) $D_m = 0$ (Aligned)



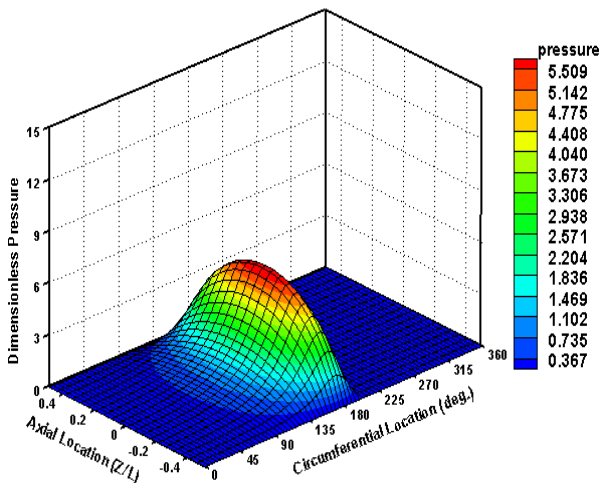
(b) $D_m = 0.4, \psi = 0^\circ$

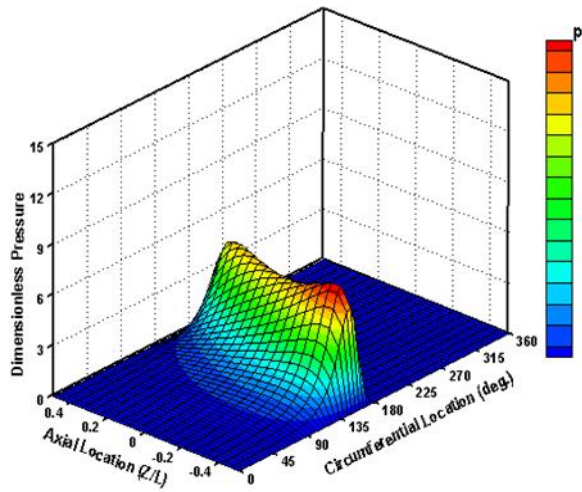


(c) $D_m = 0.4, \psi = 90^\circ$

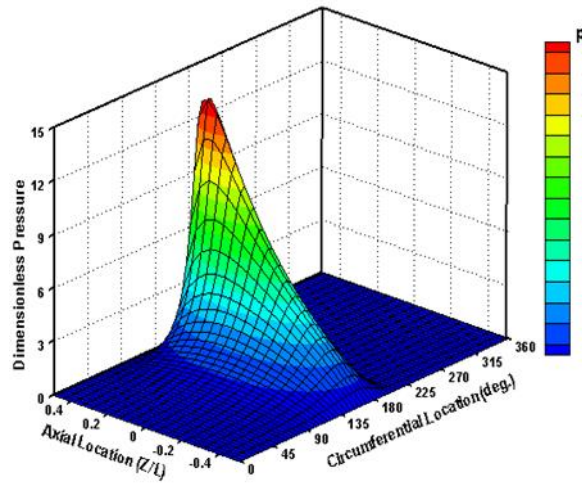


(d) $D_m = 0.8, \psi = 0^\circ$

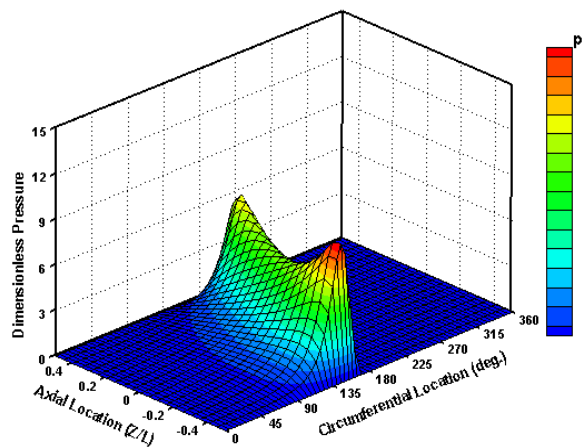




(e) $D_m = 0.8, \psi = 90^\circ$



(f) $D_m = 0.9, \psi = 0^\circ$



(g) $D_m = 0.9, \psi = 90^\circ$

Fig. 11. Variation of the dimensionless oil film pressure (\bar{P}) in the axial and

circumferential directions for different misalignment parameters with $\bar{K} = 0.001$ and $\varepsilon = 0.8$.

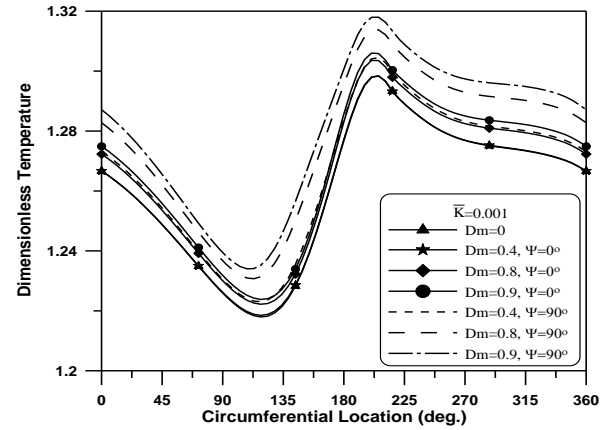


Fig. 12. Non-dimensional oil film Temperature (\bar{T}) in the circumferential direction for different misalignment parameters.

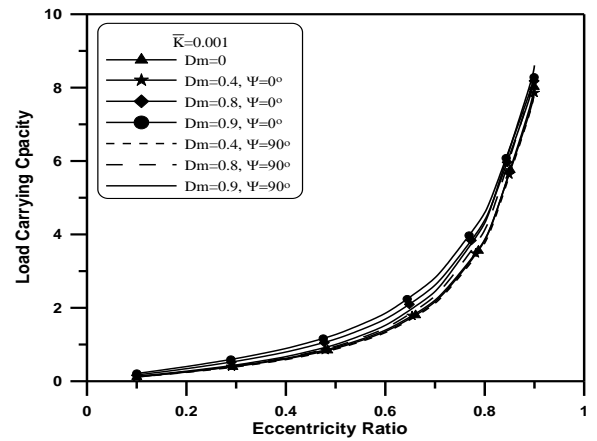


Fig. 13. Non-dimensional load carrying capacity (\bar{W}) versus eccentricity ratio for different misalignment parameters.

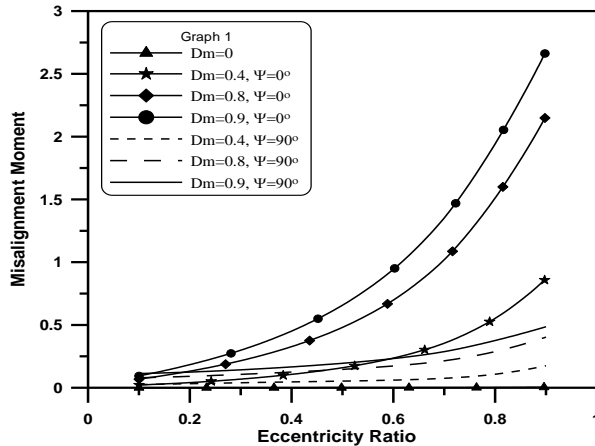


Fig. 14. Non-dimensional misalignment moment (\bar{M}) versus eccentricity ratio With different misalignment parameters.

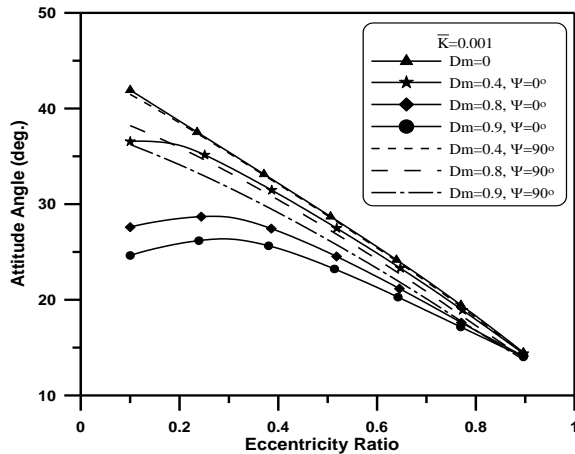


Fig. 15. Attitude angle (ϕ) versus eccentricity ratio with different misalignment parameters.

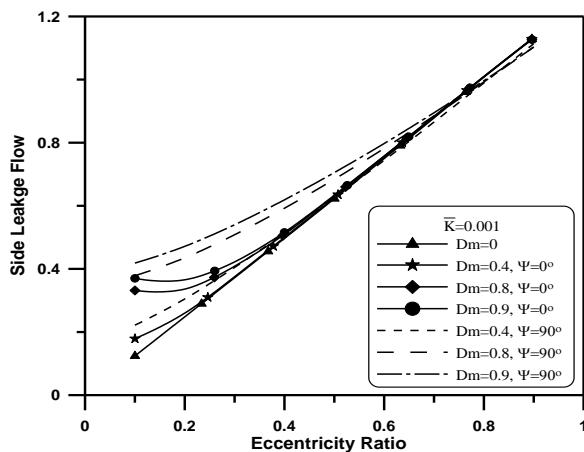


Fig. 16. Variation of Dimensionless side leakage flow with eccentricity ratio for different values of

14. Conclusions

The results presented in this study lead to the following conclusions:

1-The present model has successfully predicted the theoretical results of Boubendir et al. [8].

2-The oil film pressure, load carrying capacity and the misalignment moment are decrease for the bearing that has higher permeability parameter. A reduction of 41.8% in maximum oil film pressure has been calculated for the porous bearing that has a permeability parameter (\bar{K}) of 0.01 than that has $\bar{K}=0.0001$.

3- A little effect for the permeability of the porous bearing on the oil film temperature has been observed. A 1.5% reduction in maximum oil film temperature has been achieved.

4- The porous journal bearing that has higher permeability shows higher values of attitude angle. An increase of 8% in attitude angle has been attained for porous journal bearing that has $\bar{K}=0.001$ than that has $\bar{K}=0.0001$ when the bearing working at $\epsilon=0.7$

5- Negligible decrease in side leakage flow for the porous journal bearing that has $\bar{K}=0.0001$ to 0.001 and working at $\epsilon=0.7$. The percentage of decrease becomes 21%

for the bearing that has $\bar{K}=1$ and $\varepsilon=0.7$.

6- The minimum oil film thickness at the front side of the bearing increases when the porous bearing a higher degree of misalignment and $\psi=0$. It becomes smaller at the rear of the bearing. The minimum oil film thickness for both cases (front and rear) locates at the same position at $\theta=202^\circ$.

7- When $\psi=90^\circ$ the minimum oil film thickness decreases as the bearing has higher degree of misalignment. The minimum oil film thickness locates at $\theta=157^\circ$ in the front side while it becomes 226° at the rear side.

8- Bearing characteristics are little affected when the porous bearing has a degree of misalignment of 0.4.

9- The oil film pressure distribution shows two symmetrical pressure spikes at the front and the rear of the bearing when the bearing has $\psi=90^\circ$. A higher pressure obtained for the bearing works with higher degree of misalignment.

10- The oil film temperature is slightly affected by the bearing misalignment. A 2.3 % increase in maximum oil film temperature has been obtained when the porous bearing has $D_m=0.9$ and $\psi=90^\circ$ in comparison with aligned one.

11- The attitude angle decreases when the bearing works at

higher degree of misalignment for both cases when $\psi=0^\circ$ and 90° .

12- The oil side leakage flow of the porous bearing increases as the bearing works at higher degree of misalignment for both cases of ψ .

Nomenclature

c	Radial clearance (m)
C_p	Specific heat of pure lubricant (J/kg. °C)
D_m	Degree of misalignment
\bar{h}	Non-dimensional oil film thickness
\bar{K}	Non-dimensional permeability parameter
K_b	Thermal conductivity of the porous bush (W/m.°C)
K_f	Thermal conductivity of the lubricant (W/m.°C)
L	Bearing length (m)
\bar{M}	Non-dimensional misalignment moment.
\bar{M}_ε	Non-dimensional misalignment moment in the direction of the line of centers
\bar{M}_ϕ	Non-dimensional misalignment moment perpendicular to the line of centers.
N	Number of revolution per minute (rpm)
N_d	Dissipation number
\bar{P}	Non-dimensional oil film pressure
\bar{P}^*	Non-dimensional oil pressure inside the porous matrix
P_e	Peclet number
\bar{Q}_s	Non-dimensional Side leakage flow rate
R_s	Journal Radius (m)
R_b	Bearing (bush) radius (m)
R_{bi}	Bush inner radius (m)
R_{bo}	Bush outer radius (m)
\bar{T}	Dimensionless oil film temperature
\bar{T}_b	Dimensionless Porous bearing temperature
\bar{T}_j	Journal (shaft) temperature
T_0	Inlet temperature (°C)
U	Journal (shaft) speed (m / sec.)
\bar{u}	Dimensionless fluid velocity component in x-direction
\bar{v}	Dimensionless fluid velocity component in y-direction
\bar{w}	Dimensionless fluid velocity component in z-direction
\bar{W}	Non-dimensional load carrying capacity of

\bar{W}_ε the porous journal bearing
Non-dimensional load in the direction of the line of centers
 \bar{W}_ϕ Nondimensional load perpendicular to the line of centers.

x, y, z Coordinates system (m)

Greek Symbols

μ Lubricant viscosity (Pa.sec.)

$\bar{\mu}$ Dimensionless lubricant viscosity = $\frac{\mu}{\mu_0}$

μ_0 Inlet Lubricant viscosity (Pa.sec)

α Dimensional ratio $\alpha = \frac{R_{bi}}{L}$

β Thermo-viscous coefficient ($1/^\circ\text{C}$)

ε Eccentricity ratio

ρ Lubricant density (kg/m^3)

ϕ Attitude angle, Deg.

θ Angular coordinate, Deg.

ψ Angle between the eccentricity vector and the line of shaft projection in mid plan (Deg.)

ω Journal rotational speed (rad / sec.)

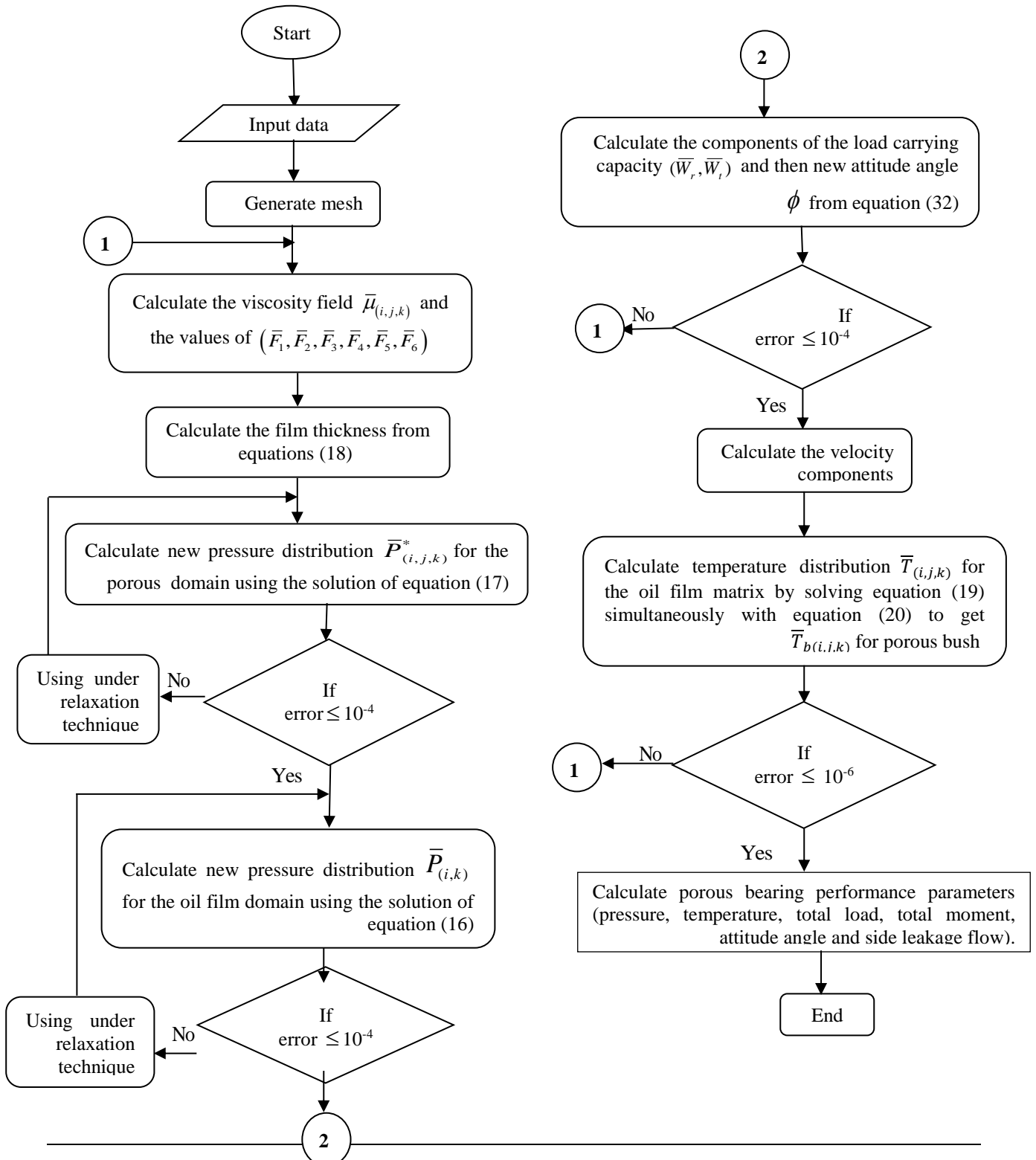
References

1. N. B. Naduvinamani and S. Santosh, "Micropolar Fluid Squeeze Film Lubrication of Finite Porous Journal Bearing" Proceedings of the 13th Asian Congress of Fluid Mechanics , pp. 970-973, 2010.
2. Lin J.R., and Hwang C. C., "Lubrication of Shaft Porous Journal Bearing-use Of The Brinkman –extended Darcy Model", Wear, Vol. 161, pp. 94-104, 1993.
3. Satoru Kaneko, Hiroyuki Takabatake and Kanya Ito, "Numerical Analysis of Static Characteristics at Start of Operation in Porous Journal Bearings With Sealed Ends", Transaction of the ASME, Vol. 121, pp. 62- 68, 1999.
4. A. A. Elsharkawy, L. Guedouar, "Hydrodynamic lubrication of porous journal bearings using a modified Brinkman-extended Darcy model" Tribology International, Vol. 34, pp. 767-777, 2001.
5. Durak Ertugrul, "Experimental Investigation of Porous Bearings Under Different Lubricant and Lubricating Conditions", KSME International Journal, 17(9), pp. 1276- 1286,2003.
6. Basim A. Abass, Alaa' M. Hussan, Lekaa' Hameed, "Operating Characteristics of Porous Floating–Ring Journal Bearings Operating with an Improved Boundary Conditions", Journal of Engineering, Vol. 13, No. 1, 2007
7. Victor G. Marian, Bernhard Scheichl, Natchana Tungkunagorn, Georg Vorlauffer and Friedrich Franek, "Evaluation of Mass Conservation Model for the Tribological Analysis of Porous Bearings", 11th International Conference on Tribology – Serbiatrib '09, pp. 220-223, 13-15, 2009.
8. Boubendir S, Larbi S, Bennacer R., "A Contribution to the Analysis of the Thermo-hydrodynamic Lubrication of Porous Self-Lubricating Journal Bearings" Defect and Diffusion Forum Vol.297, pp. 618- 623, 2010

9. S. Boubendir, S.Larbi and R.Bennacer, "Numerical study of the thermo-hydrodynamic lubrication phenomena in porous journal bearings" Tribology International, Vol. 44, pp. 1-8, 2011
10. N. S. Patel, D. P. Vakharia and G.M.Deheri, "A study on the Performance of a Magnetic Fluid based Hydrodynamic Short Porous Journal Bearing", Journal of the Serbian Society for Computational Mechanics, Vol. 6 , No. 2, pp. 28-44, 2012.
11. Ana M. Balasoiu, Minel J. Braun and Stefan I. Moldovan, "A parametric study of a porous self-circulating hydrodynamic bearing", Tribology International, PP. 176 – 193, 2013.
12. T.V. V. L. N. Roa, A. M. A. Rani, T. Nagarajan and F. M. Hashim, "Analysis of journal bearing with double- layered porous lubricant film: Influence of surface porous layer configuration" Tribology transaction, Vol. 56, pp. 864-874, 2013.
13. Oscar Pinkus and S. S. Bupara, "Analysis of Misaligned Grooved Journal Bearings", Transaction of the ASME J. Lubr. Techno., Vol. 101, PP. 503 – 508, 1979.
14. Z. S. Safar, "Energy Loss Due to Misalignment of Journal Bearing", Tribology International, Vol. 17, PP. 107 – 110, 1984.
15. Z. S. Safar and M. S. M. Riad, "Prediction of the Coefficient of Friction of A Misaligned Turbulent Flow Journal Bearing", Tribology International, Vol. 21, PP. 15 – 19, 1988.
16. T. G. Keith. JR, "Effect of Cavitation on the Performance of A Grooved Misaligned Journal Bearing", Wear, Vol. 134, PP. 377 – 397, 1989.
17. Patiala and Banwiat, "Thermo-hydrodynamic Analysis of a Misaligned Journal Bearing", Ph.D. Thesis, Deemed University,, 1998.
18. S. Boedo and J. F. Booker, "Classical Bearing Misalignment and Edge Loading: A Numerical Study of Limiting Cases", Transaction of the ASME, Vol. 126, PP. 531 – 541, 2004.
19. J. Bouyer and M. Fillon, "Influence of Deformation Effect on a Misaligned Plain Journal Bearing", World Tribology Congress III, pp. 1-2, 2005.
20. Padelis G. Nikolakopoulos and Chris A. Papadopoulos, "A study of friction in worn misaligned journal bearings under severe hydrodynamic lubrication", Tribology International, Vol.41, pp. 461–472, 2008.
21. Basim A. Abass and Mustafa Mohammed K., "The Effect of Surface Roughness on Thermo-hydrodynamic Performance in Misaligned Journal Bearings", Al-Khwarizmi Engineering Journal, Vol. 6, No.3, PP. 61-76, 2010.
22. Zhen-peng He, Jun-hong Zhang, Wei-song Xie, Zhou-yu Li and Gui-chang Zhang, "Misalignment analysis of journal bearing influenced by asymmetric

- deflection, based on a simple stepped shaft model”, Journal of Zhejiang University-Science (Applied Physics & Engineering), pp. 647-664, March 2012.
- 23 Prakash Chandra Mishra, “Mathematical Modiling of Stability in Rough Elliptic Bore Misaligned Journal Bearing Considering Thermal and Non-Newtonian Effects”, Applied Mathematical Modelling, Vol. 37, pp. 5896-5912, 2013.
- 24 Kuznetsov, E., Glavatskih, S. and Fillon, M. “THD Analysis of Compliant Journal Bearings Considering Liner Deformation”, Tribology International, Vol. 44, PP.1629–1641. 2011

Appendix (A) Program Flowchart



Yes

التحليل الحراري للمساند المقعدية ذاتية التزيت غير متطابقة المحاور

باسم عجيل عباس
مشرق علاوي مهدي
قسم الهندسة الميكانيكية / جامعة بابل / العراق

الخلاصة

يتضمن هذا البحث دراسة عددية للتحليل الحراري في المساند المقعدية ذاتية التزيت غير متطابقة المحاور. يتضمن النموذج الرياضي للعمل الحالي معادلة رينولدز المحدثة التي تحكم طبقة المائع مع الاخذ بنظر الاعتبار فقدان الزيت الى الطبقة المسامية والتي تحكم بواسطة قانون دارسي و معادلة الطاقة ومعادلة التوصيل الحراري. تم تعديل المعادلة التي استخدمت لاحتساب سمك طبقة الزيت لتأخذ بنظر الاعتبار تأثير عدم تطابق محاور المسند المقعدي المسامي. تم حل المعادلات الحاكمة مع الشروط الحدية المناسبة انياً وعددياً باستخدام طريقة الفروقات الحدية. تم تمثيل ومناقشة تأثير كل من النفاذية وحالة عدم التطابق على اداء الخصائص للمسند المقعدي المسامي. تشير النتائج المستحصلة من هذا التحليل الى ان اداء هذا النوع من المساند يتأثر بشكل كبير بهذه العوامل. تم مقارنة بعض من النتائج المستحصلة في هذا البحث مع تلك المنشورة في بحث اخر وقد اظهرت عملية المقارنة تقارباً جيداً على الموثوقية بالنموذج النظري والبرنامج الحاسوبي الذي تم اعداده لحل المعادلات الحاكمة للعمل الحالي .

الكلمات الرئيسية : الياف الجريد ; كونكريت ; الخواص الميكانيكية